

Performance Analysis of Extended Channel Models for MIMO LTE SC-FDMA Uplink Systems

P.Balasundaram, Nilkantha Chakraborty

School Of Electronics Engineering, VIT University,

Vellore-632014, Tamilnadu, India.

{lte.bala; nilkantha.chakraborty}@gmail.com

Abstract— Long Term Evolution (LTE) is the latest standard proposed by the 3GPP towards 4G. This paper uses an accurate perform analysis of complete uplink LTE study. Multiple input multiple output (MIMO) techniques have gathered much attention in recent years as a way to improve drastically the performance of wireless mobile communications. Simulated Results compare different channel estimation techniques showing significant difference among them, such as Extended Pedestrian A, Extended Vehicular A, Extended typical urban , High Speed Train Condition(HSTC) are considered and the measurement data is compared for the Localized and Distributed SC-FDMA mapping methods. From the results, we find that Localized SC-FDMA outperforms Distributed SC-FDMA in terms of SNR and BER .

Keywords— SC-FDMA, MIMO, Extended Pedestrian A, Extended Vehicular A, typical urban, Doppler Shift.

1.INTRODUCTION

The ever growing demand for multimedia services, high mobility, and global connectivity has resulted in recent years in an exploration of new technologies for wireless communication systems. Single Carrier Frequency Division Multiple Access (SC-FDMA) is a promising technique for high data rate uplink communication and has been adopted by 3GPP for its next generation cellular system, called Long-Term Evolution (LTE) [2]-[3]. SC-FDMA is a modified form of OFDM with similar throughput performance and complexity. In 3GPP Long Term Evolution (LTE), SCFDMA has been assumed for uplink transmission, whereas the Orthogonal Frequency Division Multiple Access (OFDMA) signalling format has been exploited for the downlink transmission. Thus SC-FDMA takes over all the advantages of OFDM over other well-known techniques such as TDMA and CDMA. Because broadband channels experience frequency - selective fading, the FDMA techniques can utilize both static and channel dependent scheduling to achieve multi-user diversity. The major problem in extending GSM TDMA and wideband CDMA to broadband systems is the increase in complexity with the multipath signal reception. The main advantage of OFDM, as is for SC-FDMA, is its sturdiness against multipath signal propagation, which makes it suitable for broadband systems. SC-FDMA has additional advantage of low Peak-to-Average Power Ratio (PAPR) compared with OFDM making it suitable for uplink transmission by user-equipment.

2. SYSTEM MODEL

2.1. MIMO Channel

MIMO technology leverages multipath behavior by using multiple transmitters and receivers with an added “spatial” dimension to increase performance and range. MIMO allows multiple antennas to send and receive multiple spatial streams at the same time. MIMO makes antennas work more efficiently by enabling them to combine data streams arriving from different paths and at different times to effectively increase receiver signal-capturing power.

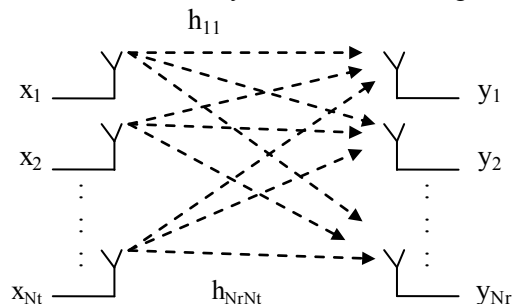


Fig.1 MIMO Channel with N_t transmitter and N_r receiver antenna

Spatial diversity technology is used by MIMO antennas. If there are more antennas than spatial streams, the additional antennas can add receiver diversity and increase range. Systems that use SISO can only send or receive a single spatial stream at one time.

To implement MIMO either mobile device or access point need to support MIMO. A MIMO system can provide two types of gain: 'spatial diversity gain' and 'spatial multiplexing gain'. Spatial diversity improves the reliability of communication in fading channels and spatial multiplexing increases the capacity by sending multiple streams of data in parallel through multiple spatial channels.

Figure 1 describe about the MIMO channel where x_1, x_2, \dots, x_{N_t} represent transmitted symbols and y_1, y_2, \dots, y_{N_r} represent received symbols. A MIMO system with Narrowband MIMO channel can be represented by the following equation

$$y = H * x + n \quad (1)$$

where y is the $N_r \times 1$ received signal vector, and H is

the $N_r \times N_t$ complex matrix of channel gains. H_{ij} representing the gain from j^{th} transmit antenna to i^{th} receive antenna. x is the $N_t \times 1$ transmitted signal vector, n is the $N_r \times 1$ zero-mean complex Gaussian noise.

$$H = UDV^H \quad (2)$$

where U is an $N_r \times N_r$ unitary matrix, D is an $N_r \times N_t$ non-negative diagonal matrix and V is an $N_t \times N_t$ unitary matrix. $(\cdot)^H$ is a Hermitian (conjugate transpose) operation. The diagonal entries of D are the nonnegative square roots of the eigen values of HH^H , the columns of U are the eigenvectors of HH^H , and the columns of V are the eigenvectors of $H^H H$.

We can rewrite Equation (1) using Equation (2) as

$$y = UDV^H x + n \quad (3)$$

Multiplying U^H on both sides of Equation (3), it becomes

$$\begin{aligned} U^H y &= U^H UDV^H x + U^H n \\ U^H y &= DV^H x + U^H n \end{aligned} \quad (4)$$

Where n has the same statistical properties as n since U is a unitary matrix. Thus n is an $N_r \times 1$ zero-mean complex Gaussian noise.

For a wideband MIMO channel, the entire band can be subdivided into subcarriers. Then, the MIMO channel for each subcarrier becomes a narrowband MIMO channel. Let the entire band be subdivided into M subcarriers, then for k^{th} subcarrier the entire band becomes a narrowband MIMO channel.

$$Y_k = H_k * X_k + N_k \quad (5)$$

where X_k is the $N_t \times 1$ transmitted signal vector, Y_k is the $N_r \times 1$ received signal vector, N_k is the $N_r \times 1$ zero-mean complex Gaussian noise, and H_k is the $N_r \times N_t$ complex matrix of channel gains H_{ij} , k representing the gain.

Spatial diversity gain is the signal-to-noise ratio (SNR) exponent of the error probability and it corresponds to the number of independently faded paths.

Alamouti transmit diversity scheme, and space-time coding are some known spatial diversity techniques. If spatial diversity is a means to combat fading, spatial multiplexing is a way to exploit fading to increase the data throughput.

Space-time block coding (STBC) technique is used to transmit multiple copies of a data stream across a number of antennas.

The transmitted signal must traverse a potentially difficult environment with scattering, refraction, reflection and then it may be corrupted by thermal noise in the receiver. So it implies that some of received copies will be better than others. In fact, space time coding combines all copies of received signal to extract information as much as possible. Alamouti transmit diversity scheme, and space-time coding are some known spatial diversity techniques. For a given MIMO channel, both diversity and multiplexing gains can be achieved simultaneously but there is a fundamental tradeoff between two gains.

2.2. SC-FDMA Signal Generation

The transmitter and receiver structure of a SC-FDMA is illustrated in Fig. 1. The Transmitter is sending multiple block of data to a receiver. The input of transmitter and the output of the receiver are complex modulation symbols. LTE systems dynamically adapt the modulation technique to the channel quality, using Binary Phase Shift Keying (BPSK) in weak channels and up to 64-level Quadrature Amplitude Modulation (64-QAM) in strong channels. The information block consists of M complex modulation symbols generated at a rate R_{source} Symbols/second. Fig. 3 provides the details of the important elements of the transmitter in Fig.2. The M - point Discrete Fourier Transform (DFT) produces M frequency domain symbols that modulate M out of N orthogonal subcarriers spread over a bandwidth.

$$W_{\text{Channel}} = N \cdot f_0 \text{ [Hz]} \quad (6)$$

Where, f_0 Hz is the subcarrier spacing. The channel transmission rate is,

$$R_{channel} = \frac{N}{M} \cdot R_{source} [symbols/second] \quad (7)$$

Bandwidth Spreading factor is given by:

$$Q = \frac{R_{channel}}{R_{source}} = \frac{N}{M} \quad (8)$$

By using above equation the SC-FDMA system can handle up to Q orthogonal source signals with each source occupying a different set of M orthogonal subcarriers.

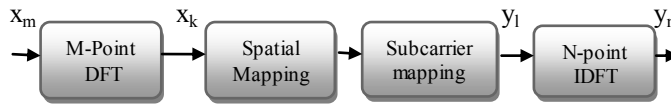


Fig.2 Generation of SC-FDMA Transmit Symbols

In the notation of Fig.2, x_m ($m = 0, 1, \dots, M - 1$) represents modulated source symbols and the DFT of x_m . Y_l ($l = 0, 1, \dots, N - 1$) represents the frequency domain samples after subcarrier mapping and y_n ($n = 0, 1, \dots, N - 1$) represents the transmitted time domain channel symbols obtained from the inverse DFT (IDFT) of Y_l . The subcarrier mapping block in Fig.2 and 3 assigns frequency domain modulation symbols to subcarriers. The mapping process, for a while referred to as scheduling. Because spatially separated terminals have independently fading channels. SC-FDMA and OFDMA can gain from channel dependent scheduling.

The inverse transform (IDFT) in Fig. 2 and 3 creates a time domain representation y_n , of the N subcarrier symbols. The transmitter in Fig. 3 inserts a set of symbols referred to as cyclic prefix (CP) in order to provide a secured guard time to prevent inter-block interference (IBI) due to multipath propagation. The transmitter also performs a linear filtering operation passed on to as pulse shaping in order to decrease out-of-band signal energy. The cyclic prefix is a copy of the last part of the block. It acts as a guard time between two consecutive blocks. Then, to remove the channel distortion by the DFT of the received signal can simply be divided by the DFT of the channel impulse response point-wise. The DFT in the receiver of Fig. 3 converts the received signal to the frequency domain in order to get better N subcarriers.

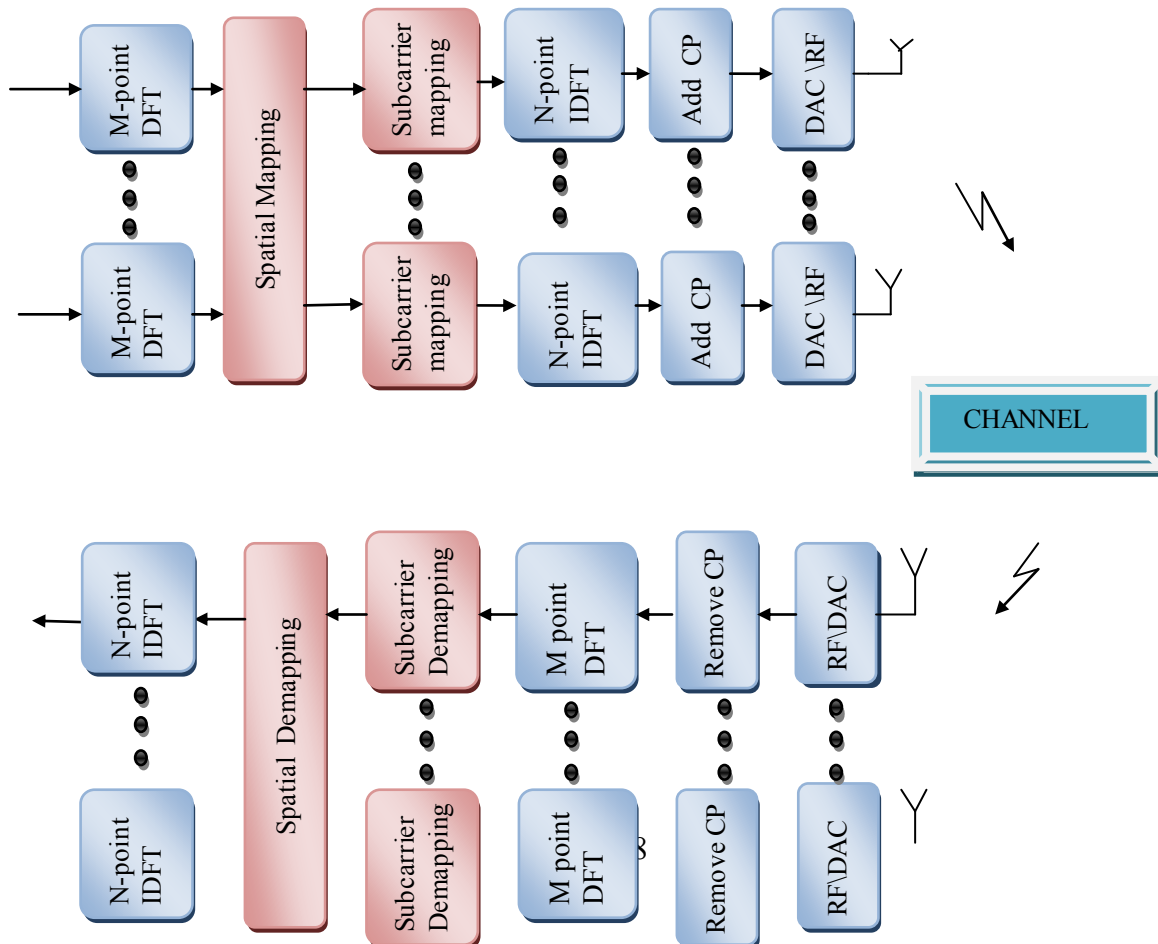




Fig. 3 Transmitter and Receiver Structure of MIMO SC-FDMA

The de-mapping operation detaches the M frequency domain samples of each source signal. Because SC-FDMA uses single carrier modulation, it runs into the substantial linear distortion manifested as inter-symbol interference (ISI). The frequency domain equalizer cancels the ISI. The IDFT in the receiver of Fig. 3 transforms frequency equalized symbols back to the time domain, where a detector produces the received sequence of M modulation symbols.

2.3. Subcarrier Mapping

Fig.4 and Fig.5 show two methods of mapping the M frequency domain modulation symbols to subcarriers: distributed and localized subcarrier mapping. In localized subcarrier mapping mode, the modulation symbols are allocated to M adjacent subcarriers. In the distributed mode, the symbols are equally spaced across the entire channel bandwidth. In both modes, the IDFT in the transmitter assigns zero amplitude to the N – M unoccupied subcarriers. The localized and distributed subcarrier mapping methods are also referred to as localized FDMA (LFDMA) and distributed FDMA (DFDMA).

The case of N=Q×M for the distributed mode with equidistance between occupied subcarriers is referred to as Interleaved FDMA (IFDMA). IFDMA is a special case of SC-FDMA and it is very efficient in that transmitter can modulate the signal firmly in the time domain without the use of DFT and IDFT. In this paper only LFDMA and DFDMA are considered for the analysis of mobile radio channels.

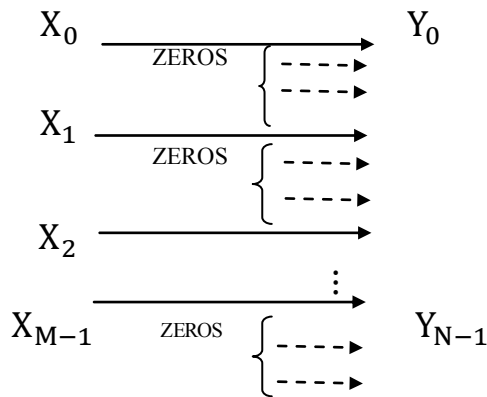


Fig. 4 Distributed Mapping

The time domain samples of DFDMA signal can be expressed as below,

$$Y_n = Y_{Qm+q}$$

$$= \begin{cases} \frac{1}{Q} X_{n(Q \bmod M)} \bmod M, & q = 0 \\ \frac{1}{Q} \cdot \left(1 - e^{j 2\pi \frac{Q}{Q} q}\right) \cdot \frac{1}{M} \sum_{p=0}^{M-1} \frac{x_p}{1 - e^{j 2\pi \left(\left(\frac{Qm-p}{M}\right) + \frac{Qq}{QM}\right)}}, & q \neq 0 \end{cases} \quad (9)$$

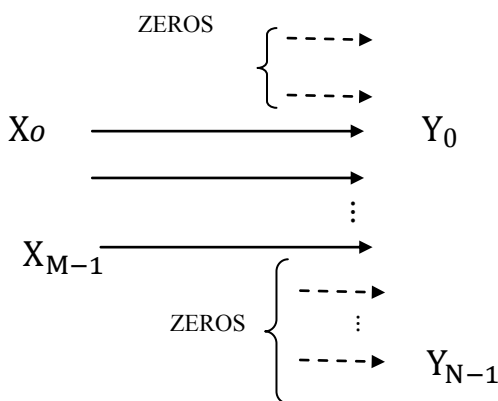


Fig. 5 Localized Mapping

The time domain samples of the LFDMA signal can be expressed as below,

$$Y_n = Y_{Qm+q}$$

$$= \begin{cases} \frac{1}{Q} X_{n \bmod M}, & q = 0 \\ \frac{1}{Q} \cdot \left(1 - e^{j 2\pi q/Q}\right) \cdot \frac{1}{M} \sum_{p=0}^{M-1} \frac{x_p}{1 - e^{j 2\pi \left(\left(\frac{m-1}{M}\right) + \frac{q}{QM}\right)}}, & q \neq 0 \end{cases} \quad (10)$$

2.4. High Speed Train Condition

Doppler Shift has major effect in case of high speed train condition. The Doppler effect (or Doppler shift), is the change in frequency of a wave for an observer moving relative to the source of the wave. When a vehicle sounding a siren approaches, passes, and recedes from an observer, the received frequency is higher (compared to the emitted frequency) during the approach, it is identical at the instant of passing by, and it is lower during the recession.

The high speed train conditions for the test of the baseband performance are two non-fading propagation channels. For BS with Rx diversity, the Doppler shift variation is the same between antennas.

Doppler shift is given by:
$$f_s(t) = f_d(t) \cos\theta(t); \quad (11)$$

Where $f_s(t)$ is the Doppler shift and f_d is the maximum Doppler frequency. $D_s/2$ is the initial distance of the train from BS, and D_{min} is BS-Railway track distance, both in meters; v is the velocity of the train in m/s, t is time in seconds.

TABLE 1
HIGH SPEED TRAIN CONDITION

Parameter	Scenario1	Scenario2
D_s	1000m	300m
D_{min}	50m	2m
V	350km/hr	300km/hr
f_d	1340hz	1150hz

3. PERFORMANCE ANALYSIS OF MULTI-PATH PROPAGATION CHANNELS

The multipath propagation condition consists of several parts:

- A delay profile in the form of a “tapped delay-line”, characterized by a number of taps at fixed positions on a sampling grid. The profile can be further characterized by the r.m.s delay spread and the maximum delay spanned by the taps.
- A combination of channel model parameters that include the Delay profile and Doppler spectrum that characterized by a classical spectrum shape and a maximum Doppler frequency.

In this paper, both delay profiles and Doppler spectrum for various E-UTRA channel models were considered. The delay profiles are selected to be representative of low, medium and high delay spread environments. The resulting model parameters are defined in Table 2.

Here the Excess tap delay and Relative power were analysed and the mobile radio channels such as Extended Pedestrian A, Extended Vehicular A, Extended typical urban Model and HSTC model performance were compared using the Table (2, 3,4).

TABLE 2
DELAY PROFILES FOR E-UTRA CHANNEL MODELS

Model	No. of channel taps	Max. delay
Extended Pedestrian A (EPA)	7	410 ns
Extended Vehicular A (EVA)	9	2510 ns
Extended typical urban (ETU)	9	5000 ns

EPA		EVA	
Excess tap delay(ns)	Relative power (dB)	Excess tap delay(ns)	Relative power (dB)

AND

EXTENDED

0	0	0	0
30	-1	30	-1.5
70	-2	150	-1.4
90	-3	310	-3.6
110	-8	370	-0.6
190	-17.2	710	-9.1
410	-20.8	1090	-7
-	-	1730	-12

TABLE 3
EXTENDED PEDESTRIAN A
VEHICULAR A MODEL

TABLE 4
EXTENDED URBAN AND HSTC MODEL

ETU		HSTC Model	
Excess tap delay(ns)	Relative power (dB)	Excess tap delay(ns)	Relative power (dB)
0	-1	0	-1
50	-1	900	-21
120	-1	1900	-35
200	0	2200	-39
230	0	2700	-39.1
500	0	6100	-43
1600	-3	7100	-21.2
2300	-5	10100	-35
5000	-7	-	-

Table 5 shows channel propagation conditions that are used for the performance measurements in multi-path fading environment for low, medium and high Doppler frequencies. In this paper, the combination of channel models that include the Delay profile and the Doppler spectrum are considered for the simulation [5].

TABLE 5
CHANNEL MODEL PARAMETERS

Model	Maximum Doppler Frequency
EPA	5Hz
EVA	70Hz

ETU	300Hz
HSTC	1340Hz

Table (2 & 3) shows multi-path delay profiles that are used for the performance measurements in multi-path fading environment. The Excess tap delay functions can be expressed in terms of Doppler spectrum as mentioned below.

$$S(f) \propto \frac{1}{\sqrt{1 - \left(\frac{f}{f_d}\right)^2}} \quad (12)$$

Where, S (f) - Doppler spectrum,
f - Frequency,
f_d - Doppler frequency.

4. SIMULATION RESULTS AND DISCUSSION

TABLE 6

ASSUMPTIONS AND PARAMETERS

SIMULATION

System bandwidth	5MHz
Sampling rate	5 mega-samples per second
Modulation	QPSK
Cyclic prefix	20 samples (4 μs)
IFFT size	1024
Subcarrier spacing	4.882 kHz (=5MHz/1024)
Transmitter antenna	2
Receiver antenna	2
Input Block size	32 symbols
Channel estimation	Perfect
Equalization	MMSE
Channel model	Extended Pedestrian A Extended Vehicular A Extended Typical Urban HSTC model

The above mentioned parameters are used for obtaining the results, specified in the Fig. (6, 7, 8, 9).

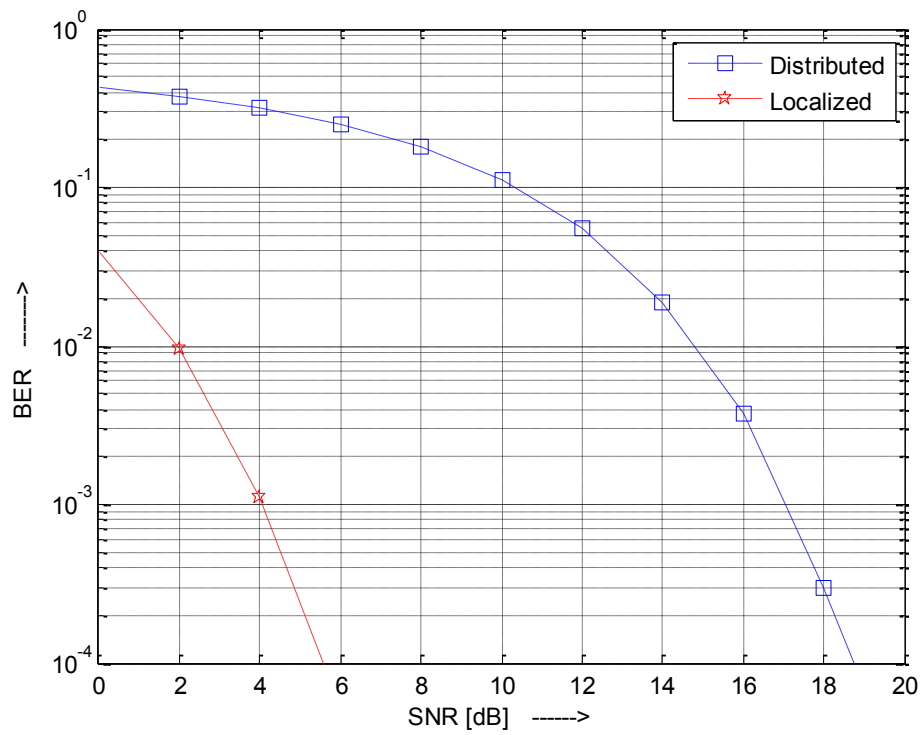


Fig. 6 Performance of Extended Pedestrian-A Channel

Extended Pedestrian A model, extended to a wider bandwidth of 20 MHz and the channel model represents a User Equipment (UE) speed of 3 km/h. EVA model, extended to a wider bandwidth of 20 MHz and the channel model represents UE speeds of 30, 120 km/h and higher values.

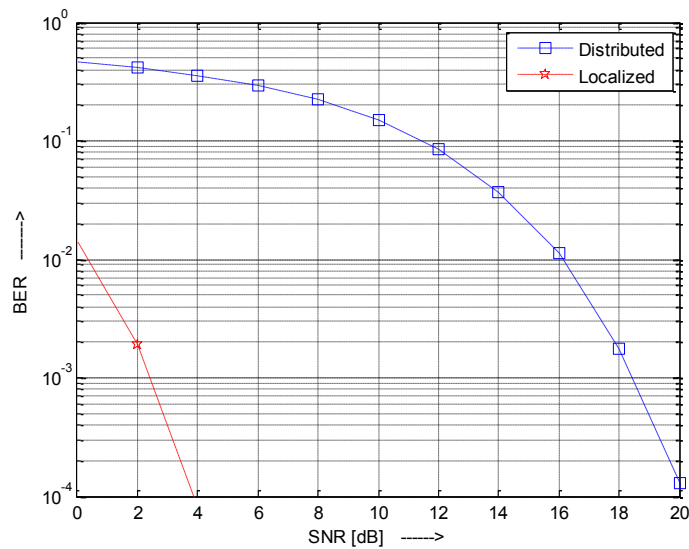


Fig. 7 Performance of Extended Vehicular-A Channel

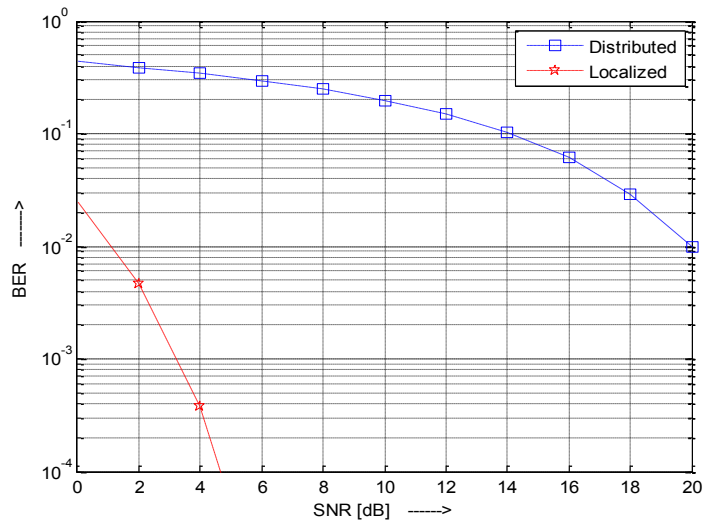


Fig.8 Performance of Typical Urban Model

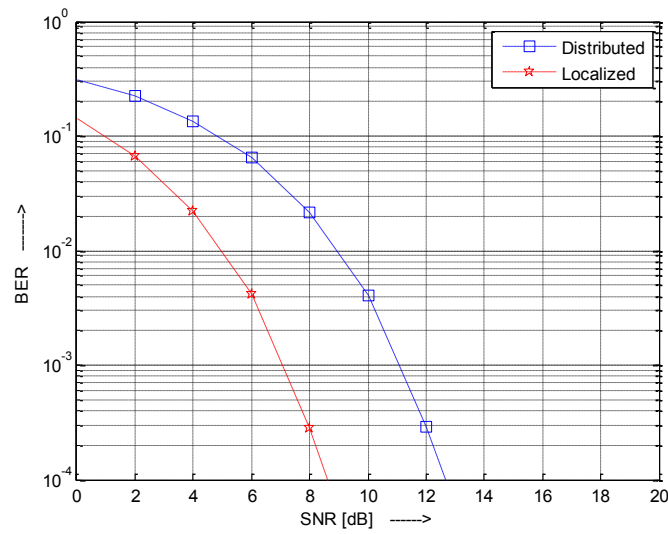


Fig.9 Performance of HSTC Model

In the case of Extended Pedestrian A, Extended Vehicular A and Typical Urban (Fig. 6, 7, 8) the Number of channel taps will be increased and simultaneously the maximum Delay will also get increased.

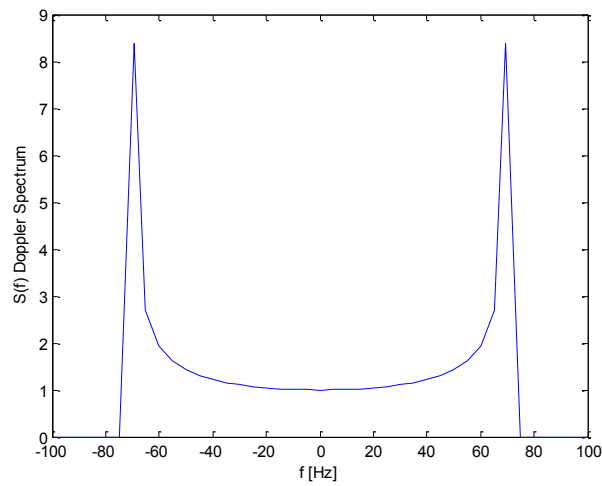


Fig.10 The Classical Doppler Spectrum EVA for 70Hz

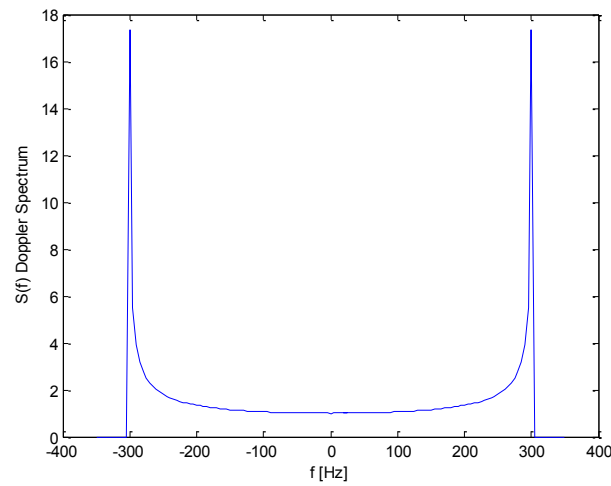


Fig.11 The Classical Doppler Spectrum ETU for 300 Hz

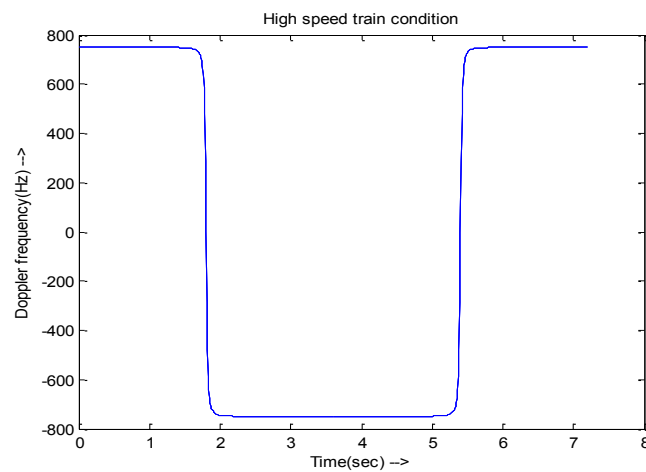


Fig.12 Doppler shift trajectory for HSTC model

The mobile Broadband single carrier signals of SC-FDMA have complex sinusoidal components spanning up to 20MHz. From the above Fig.10 & 11, it is clear that the receiver signal has components at a band of frequencies offset from the original by frequencies between -500 Hz to 500 Hz. Fig.12 is simulated result of the mathematical expression for High Speed Train . This result helps to obtain the performance of HSTC model.

5. CONCLUSION

In this paper, the LTE MIMO uplink scenario is taken up for the mobile radio transmission channels such as Extended Pedestrian A, Extended Vehicular A, Extended typical urban , High Speed train condition and the measurement data has been applied and compared for the Localized and Distributed SC-FDMA mapping methods. As per our simulation results, we found that Localized mapping gives better performance in terms of SNR and BER, when compared with Distributed SC-FDMA.

REFERENCES

- [1] S.Sesia.et al., LTE-The UMTS Long Term Evolution: From Theory to Practice, UK: John Wiley & Sons, 2009.
- [2] Hyung G.Myung and David J.Goodman, "Single Carrier-FDMA: A New Sir Interface for Long Term Evolution," UK: John Wiley & Sons, 2008.
- [3] 3GPP TS 36.101 v9.4.0 (2010-06), "Evolved Universal Terrestrial Radio Access (E-UTRA), User Equipment (UE) radio transmission and reception".
- [4] 3GPP TS 36.211 v9.1.0 (2010-04), "Evolved Universal Terrestrial Radio Access (E-UTRA), Physical channels and modulation".
- [5] 3GPP TS 36.141 v9.4.0 (2010-07), "Evolved Universal Terrestrial Radio Access (E-UTRA), Base Station(BS) conformance testing
- [6] Hyung G.Myung, David J.Goodman, "Single Carrier-FDMA for Uplink Wireless Transmission," IEEE Transactions on Vehicular Technology, vol.1, pp.30-38, September.2006.